Article

Neuron

Single Neurons in the Human Brain Encode Numbers

Highlights

- Single neurons in the human medial temporal lobe (MTL) encode numerical information
- Numerosity and abstract numerals are encoded by distinct neuronal populations
- Numerosity representation shows a distance effect; numerals are encoded categorically
- Representation of symbolic numerals may evolve from numerosity representations

Authors

Esther F. Kutter, Jan Bostroem, Christian E. Elger, Florian Mormann, Andreas Nieder

Correspondence

florian.mormann@ukbonn.de (F.M.), andreas.nieder@uni-tuebingen.de (A.N.)

In Brief

Kutter et al. show how nonsymbolic and symbolic numerical quantity is encoded in the human brain by neurons of the medial temporal lobe. The data support the hypothesis that high-level human numerical abilities are rooted in biologically determined mechanisms.

Kutter et al., 2018, Neuron *100*, 753–761
November 7, 2018
https://doi.org/10.1016/j.neuron.2018.08.036

CellPress

Neuron
Article

Single Neurons in the Human Brain Encode Numbers

Esther F. Kutter,[1,2] Jan Bostroem,[3] Christian E. Elger,[1] Florian Mormann,[1,4,*] and Andreas Nieder[2,4,5,*]
[1]Department of Epileptology, University of Bonn Medical Center, Sigmund-Freud-Str. 25, 53105 Bonn, Germany
[2]Animal Physiology Unit, Institute of Neurobiology, University of Tübingen, 72076 Tübingen, Germany
[3]Department of Neurosurgery, University of Bonn Medical Center, Sigmund-Freud-Str. 25, 53105 Bonn, Germany
[4]Senior author
[5]Lead Contact
*Correspondence: florian.mormann@ukbonn.de (F.M.), andreas.nieder@uni-tuebingen.de (A.N.)
https://doi.org/10.1016/j.neuron.2018.08.036

SUMMARY

Our human-specific symbolic number skills that underpin science and technology spring from nonsymbolic set size representations. Despite the significance of numerical competence, its single-neuron mechanisms in the human brain are unknown. We therefore recorded from single neurons in the medial temporal lobe of neurosurgical patients that performed a calculation task. We found that distinct groups of neurons represented either nonsymbolic or symbolic number, but not both number formats simultaneously. Numerical information could be decoded robustly from the population of neurons tuned to nonsymbolic number and with lower accuracy also from the population of neurons selective to number symbols. The tuning characteristics of selective neurons may explain why set size is represented only approximately in behavior, whereas number symbols allow exact assessments of numerical values. Our results suggest number neurons as neuronal basis of human number representations that ultimately give rise to number theory and mathematics.

INTRODUCTION

Numbers are fundamental to science and technology. Despite counting and arithmetic requiring years of training, the origins of our symbolic number capabilities are deeply rooted in our ancestry (Dehaene, 1997). Human adults without formal education (Gordon, 2004; Pica et al., 2004), pre-linguistic human infants (Wynn, 1992; Xu and Spelke, 2000), and nonhuman animals (Brannon and Terrace, 1998; Scarf et al., 2011) can approximately estimate numerosity, the number of items in a set. These intuitive nonsymbolic capabilities are harnessed and qualitatively transformed by children when they begin to learn symbolic counting and mathematics in school (Halberda et al., 2008; Gilmore et al., 2010; Starr et al., 2013). This intimate relationship between set size estimation and precise counting suggests that symbolic arithmetic abilities build on nonsymbolic numerical capacities.

Studies in humans (Piazza et al., 2007; Arsalidou and Taylor, 2011) and nonhuman primates (Nieder, 2016) indicated parts of the parietal and prefrontal cortices as a core number system that processes nonsymbolic and symbolic numerical magnitude. However, the wider cortical number network also incorporates areas of the medial temporal lobe (MTL) (Menon, 2016), such as the hippocampus, parahippocampal cortex, entorhinal cortex, and amygdala. The MTL comprises highly associative brain areas that are directly and reciprocally connected with the frontal number network (Goldman-Rakic et al., 1984), and human MTL neurons are known for their selectivity to abstract categories (Quiroga et al., 2005; Mormann et al., 2011). Functional imaging studies in humans showed that the hippocampal system—among many other functions outside of the number domain—is also involved in learning to count and arithmetic skill acquisition, specifically during childhood (De Smedt et al., 2011; Supekar et al., 2013; Qin et al., 2014). Hippocampal-frontal circuit reorganization plays an important role in children's shift from effortful counting to efficient memory-based solving of mathematical problems (Menon, 2016).

As a neuronal correlate of numerosity representations, electrophysiological recordings from the association cortex of monkeys showed neurons that are tuned to a specific preferred numerosity of visual and auditory items. Such number neurons have also been postulated by neural network models (Dehaene and Changeux, 1993; Verguts and Fias, 2004). In humans, number neurons have been suggested based on blood flow changes in functional imaging studies (Piazza et al., 2004; Jacob and Nieder, 2009a), as well as the combined synaptic mass signals from hundreds of neurons measured with electrocorticography (ECoG) (Daitch et al., 2016). Despite the progress that has been made using functional imaging and ECoG recordings, the mechanism of how single neurons, the anatomical and functional units of the brain, encode nonsymbolic or symbolic numerical information in humans remains unknown. We addressed this question and recorded from single neurons in the MTL of neurosurgical patients that performed a calculation task and were implanted with intracranial electrodes (Fried et al., 1997; Kreiman et al., 2000; Reber et al., 2017).

RESULTS

Participants performed simple sequential addition and subtraction tasks using a computer display (Figure 1A). Task involvement ensured that numbers shown as operands were

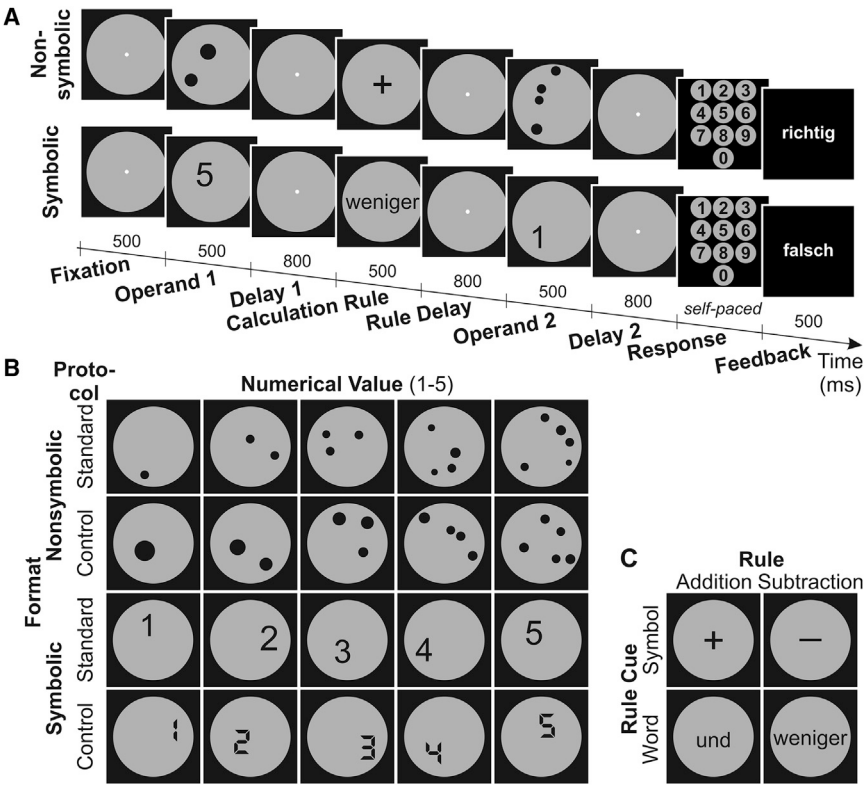

Figure 1. Behavioral Task and Example Stimuli

(A) Experimental design of the calculation task. After visual fixation on the screen, the first number (operand 1) was followed by a brief delay, after which the addition or subtraction rule was presented, followed in turn by a delay and then the second number (operand 2). After another brief delay, subjects were required to indicate the calculated result (ranging from 0 to 9) on a number panel.

(B) Example operand 1 stimuli for the nonsymbolic and symbolic format for standard and control protocols.

(C) Example stimuli for the different calculation rules indicated by arithmetic symbols ("+" and "−") and written words ("und" [add] and "weniger" [subtract]), respectively.

consciously processed. Numerical values of the operands ranged from 1 to 5. In half of the shuffled trials, the numerical values were presented nonsymbolically as the number of randomly placed dots in an array (numerosity). In the other half, Arabic numerals were shown as symbolic number representations. Both nonsymbolic and symbolic numbers were shown in standard and control displays in order to control for low-level visual features (Figure 1B; see Supplemental Information). Arithmetic symbols or words were applied for addition and subtraction instructions (Figure 1C). Average performance of all participants was close to ceiling for all tested quantities and calculations (performance range 90.3%–99.8%).

We recorded from 585 single neurons in the medial temporal lobes (153 amygdala, 126 parahippocampal cortex, 107 entorhinal cortex, and 199 hippocampus) of nine human subjects performing the calculation tasks. In order to explore pure number representations, and to avoid confounds with cognitive factors later in the task, we focus on the presentation of the first operand (operand 1) and the subsequent working memory phase (delay 1); the remaining task phases are considered toward the end of the results. Random presentation of either the nonsymbolic or symbolic format from trial to trial allowed us to investigate an individual neuron's responses to each of the formats individually, but also to both formats, in an unbiased way.

Single Neurons Encode Nonsymbolic Number

When the participants calculated with numerosities (nonsymbolic format), a substantial proportion of the tested neurons (16%; $p << 0.001$ in binomial test; $p_{chance} = 0.01$; see also Supplemental Information for verification with shuffled data) showed activity that varied exclusively with the number of items during operand 1 presentation and the working memory delay 1 that followed, irrespective of the dot array layout (2-factor sliding-window ANOVA, with factors "numerical value" × "protocol"; $\alpha = 0.01$; Figure S1, left). Four of such numerosity-selective neurons are shown in Figure 2, left column. Each cell is tuned to numerosity; it shows peak activity for one of the numerosities, its preferred numerosity, and a systematic decrease of activity the more the number of items deviates from the preferred value. The highest fraction of such numerosity-selective neurons in the MTL was found in the parahippocampal cortex (29%), followed by the hippocampus (18%; Figure 3, upper columns). The selective neurons' preference covered the entire tested range of numerosities, albeit with most neurons preferring numerosity "five" (Figure 4A, left). The proportion of neurons selective to nonsymbolic number for each subject is shown in Table S1. Firing rates were generally low in the MTL, but the firing rates of numerosity-selective neurons were significantly higher compared to the non-selective neurons ($p < 0.0001$; Mann-Whitney U test; Figure S2, left).

Average tuning curves were calculated by averaging the normalized activity for all numerosity-selective neurons that preferred a given numerosity. Neural activity formed overlapping tuning functions with progressively reduced activity as distance from the preferred quantity increased (Figure 4B, left). To compare the decay of activity from the preferred quantity across all neurons tuned to preferred numerosities 1–5, we plotted the normalized firing rates as a function of absolute numerical distance from the preferred numerosity. For example, the normalized firing rate to numerosity 2 and 4 of a cell tuned to numerosity 3 (3 therefore is absolute numerical distance 0) were plotted at absolute numerical distance 1. The pooled function for all selective neurons compared to a function from random tuning curves is shown in Figure 4C, left. On average, activity dropped off progressively with numerical distance across all preferred numerosities, an effect that is not observed for random tuning curves. This

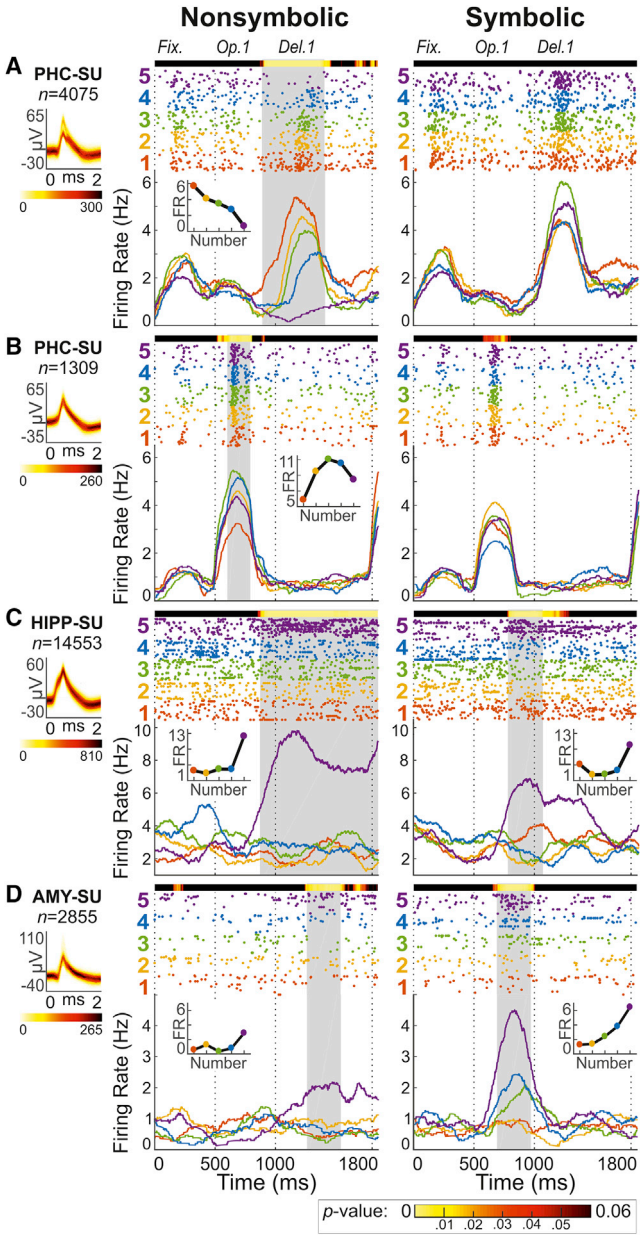

Figure 2. Neural Responses of Number-Selective Neurons during Presentation of Operand 1 and Delay 1

Responses of four example neurons to both nonsymbolic numerosities (left column) and symbolic numerals (right column). The left panels depict a density plot of the recorded action potentials (color darkness indicates number of overlapping wave forms according to color scale at the bottom). Panels show single-cell response rasters for many repetitions of the format (each dot represents an action potential) and averaged instantaneous firing rates below. The first 500 ms represent the fixation period. Colors correspond to the five different operand 1 values. Gray shaded areas represent significant number discrimination periods according to the sliding-window ANOVA (color-coded p values above each panel). Insets show the number tuning functions.

(A and B) Two parahippocampal neurons only responsive to nonsymbolic number with preferred numerosity 1 (A) and 3 (B).

(C and D) Hippocampal neuron #1 (C) and neuron #2 (D) responding to both nonsymbolic and symbolic number 5.

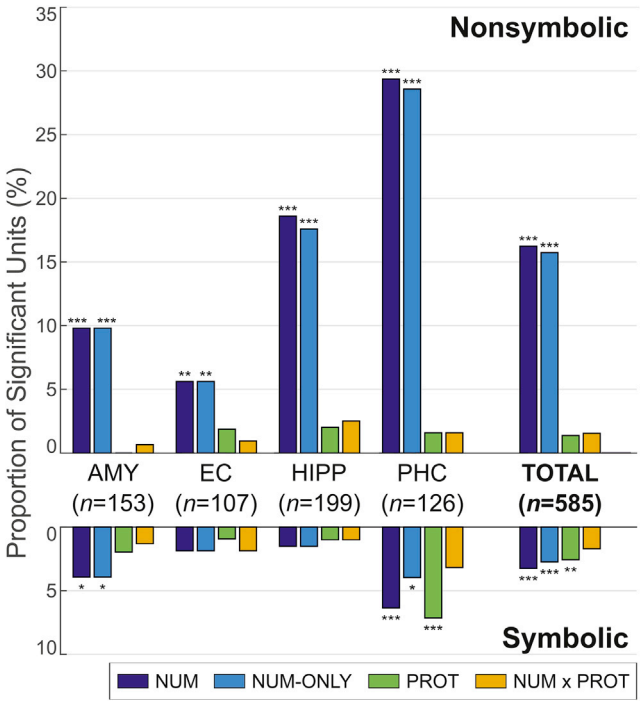

Figure 3. Neuronal Selectivity of MTL Single Units

Proportions of single units with significant main effects for "numerical value" (NUM: 1–5) or "protocol" (PROT: standard and control) and interactions (NUM × PROT) in a 2-factor ANOVA evaluated at $\alpha = 0.01$, separately for each format and MTL region (AMY, amygdala; EC, entorhinal cortex; HIPP, hippocampus; PHC, parahippocampal cortex). All analyses refer to exclusively number-selective (NUM-ONLY) units, i.e., neurons with an effect for numerical value but no concurrent effects for protocol or interaction. Numbers of significant neurons were subjected to a Bonferroni-corrected (n = 4) binomial test; asterisks indicate significance (*p < 0.05, **p < 0.01, and ***p < 0.001).

finding reflects a neuronal correlate of the well-known "numerical distance effect," the behavioral observation that discrimination progressively enhances as numerical distance between two quantities increases (Buckley and Gillman, 1974; Merten and Nieder, 2009). A cross-validation analysis (see Supplemental Information) yielded high reproducibility of preferred numerosity for the population of numerosity-selective units (average correlation coefficient $r = 0.83$; $p < 0.0001$), indicating that the preferred numerosity of the neurons was reliable and robust.

Single-Cell Responses to Symbolic Number

When participants calculated with Arabic numerals (symbolic format), a smaller but significant proportion of the recorded neurons (3%; $p < 0.001$ in binomial test; $p_{chance} = 0.01$) responded selectively to numerals during operand 1 presentation and the subsequent working memory delay 1 (2-factor sliding-window ANOVA, with factors numerical value × protocol; $\alpha = 0.01$; Figure S1, right). The highest fraction of such numeral-selective neurons in the MTL was again found in the parahippocampal cortex (6%), followed by the amygdala (4%; Figure 3, lower columns). Six numeral-selective neurons (1% of all neurons) were also tuned to nonsymbolic number, which was more than

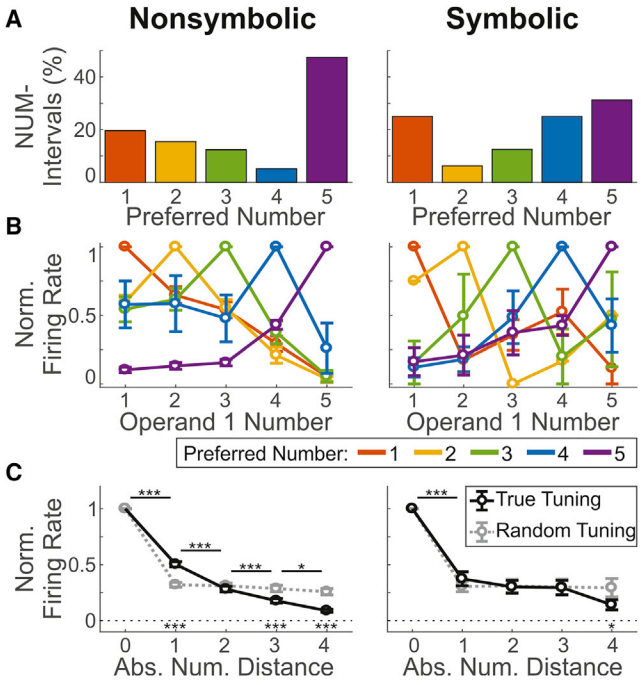

Figure 4. Tuning Properties of Number-Selective Neurons

(A) Frequency distribution of the preferred number of neurons tuned to numerosity (left) and numerals (right).

(B) Average tuning curves of neurons tuned to the five numerosities (left) and numerals (right).

(C) Averaged normalized activity across all preferred numerosities (left) and numerals (right) as a function of absolute numerical distance (black line). Asterisks above the graph represent significant differences between responses to adjacent numerical distances; asterisks below the dashed line indicate significant differences between recorded and random tuning curves (*$p < 0.05$ and ***$p < 0.001$). Error bars denote SEM.

expected by chance ($p < 0.05$ in binomial test; $p_{chance} = 0.16 \times 0.03 = 0.005$, or 0.5%). Of these, four neurons had identical preferred numerical values for nonsymbolic and symbolic number. This correlation did not reach significance (Figure S3A), possibly due to the small sample size. Next, we investigated whether the preferred numbers of units tuned to nonsymbolic numerosity might be correlated with their (non-significant) tuning to symbolic numerals (Figure S3B) and vice versa (Figure S3C). Neither correlation reached significance, indicating that numerosity and abstract numerals are encoded by two largely distinct neuronal populations. Two neurons tuned to the same value in both nonsymbolic and symbolic formats are depicted in Figures 2C and 2D. The neuron in Figure 2C as well as the neuron in Figure 2D showed maximum responses to quantity 5 in both the nonsymbolic and symbolic format. In contrast, the two neurons shown in Figures 2A and 2B were only significantly tuned to dot numerosities, but not to numerals. Again, a cross-validation analysis confirmed the reliability of the preferred numeral determination (average correlation coefficient $r = 0.57$; $p < 0.05$). The proportion of neurons selective to symbolic number for each subject is shown in Table S1. As for nonsymbolic number, the firing rates of numeral-selective neurons were significantly higher compared to the non-selective neurons ($p < 0.01$; Mann-Whitney U test; Figure S2, right).

Overall, the numeral-selective neurons' preference covered the entire range of numbers 1–5 (Figure 4A, right), and their normalized activity for each preferred numeral formed overlapping tuning functions (Figure 4B, right). The decline of activity from the preferred to the nonpreferred numerals was brisk and categorical, with only a mild progressive decrease with numerical distance, hardly showing a neuronal numerical distance effect (Figure 4C, right). At absolute numerical distance 1, the normalized firing rates obtained for symbolic number (n = 16) were significantly lower compared to nonsymbolic number (n = 92; $p < 0.05$; t test), indicating higher selectivity for (or sharper tuning to) symbolic number. When comparing the neuronal latencies to reach number-selectivity, neurons tuned to nonsymbolic (990 ms) and symbolic number (880 ms) did not differ significantly ($p = 0.23$; Mann-Whitney U test).

Neuronal Population Coding

So far, our data suggest two main findings at the level of individual neurons. First, the representation of nonsymbolic number was abundant and comparable to the core number network in nonhuman primates (Nieder et al., 2002, 2006; Nieder and Miller, 2004), whereas the representation of symbolic numbers was sparse in the MTL. Second, neurons responsive to nonsymbolic or symbolic number formats are largely segregated in the MTL; abstract neurons that encode the same numerical value in both nonsymbolic and symbolic formats were rarely found.

We therefore explored how the two populations of numerosity-selective and numeral-selective neurons encode numerical values. To evaluate the neuronal populations' information carried about number, we first trained a multi-class support vector machine (SVM) classifier to discriminate numerical values based on the spiking activity of selective MTL neurons (see Supplemental Information). After training, the classifier was tested with novel data from the same neuronal population to explore how well it could predict number categories based on the information extracted from trials used for classifier training. Initially, we performed a temporal cross-training classification to assess the classifier's accuracy in identifying the correct numerical values when tested on the activity from a given time period after being trained on other time periods of the trials. With a chance performance of 20% (for five classes), the classifier accuracy was significantly higher for both nonsymbolic and symbolic number throughout the operand 1 and delay 1 phases, albeit with better performance during the nonsymbolic-format trials (Figures 5A and 5B).

Next, we trained and tested the classifier on the firing rates of each neuron obtained by averaging across the time window that had turned out significant in the cross-training classification. The resulting confusion matrices show robust accuracy (65.6% ± 2.5%) for the five numerosities in the nonsymbolic format represented by the diagonal (Figure 5C, left). The probability of misclassification of trials increased the closer two classes were in the numerical space ("distance effect"; Figure 5D, left). Also for number symbols, the numerical values could be classified significantly above chance level but with lower accuracy (38.8% ± 2.9%; Figure 5C, right). Misclassifications hardly varied

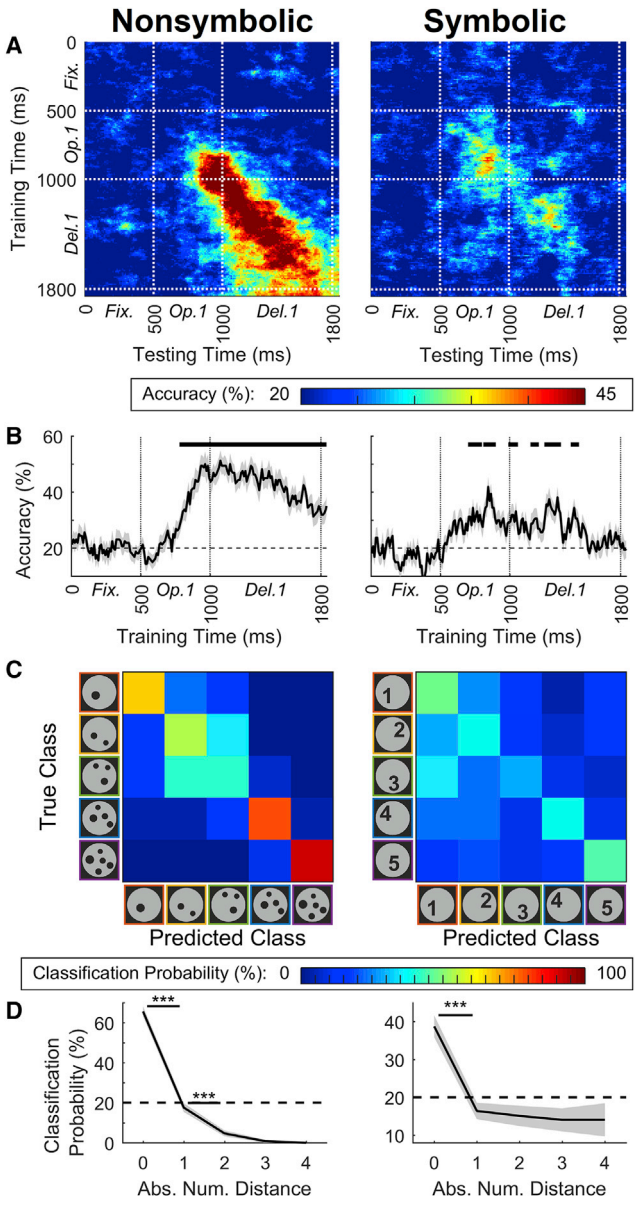

Figure 5. Numerosity Decoding Using a SVM Classifier

(A) Classification accuracy for decoding numerosity information when training a multi-class support vector machine (SVM) on instantaneous firing rates at a given time point and testing on another one for numerosity-selective (left) and numeral-selective (right) neurons.

(B) Accuracy for training and testing on identical time periods (main diagonal of matrices in A). The dashed line represents chance level (20% for five classes). Black bars above the data indicate significance ($p < 0.01$) when testing against performance for SVMs trained on shuffled data in a permutation test. Shaded areas indicate SEM.

(C) Confusion matrix derived when training an SVM on firing rates, averaged across the significant time windows in the temporal cross-training classification (B). Values on the main diagonal represent correct classification.

(D) Classification probability as a function of numerical distance. The dashed line represents chance level; shaded areas indicate SEM; asterisks represent significant differences between adjacent numerical distances ***$p < 0.001$).

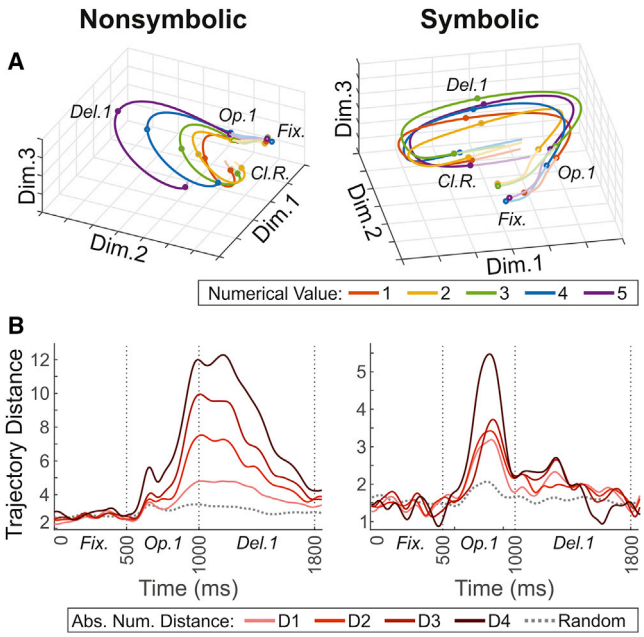

Figure 6. Population Dynamics based on State-Space Analysis

(A) Average state-space trajectories, reduced to the three principal dimensions for visualization, for the sub-populations of numerosity-selective (left) and numeral-selective (right) units. Each trajectory depicts the temporal evolution in the time window 0–1,850 ms. Circles indicate boundaries between experimental periods (*Cl.R.*, calculation rule; *Del.1*, delay 1; *Fix.*, fixation; *Op.1*, operand 1).

(B) Intertrajectory distances, averaged across pairs of trajectories with the same numerical distance. Dashed lines represent the average distances for trajectories obtained for label-shuffled data.

as a function of numerical distance for number symbols (Figure 5D, right). At absolute numerical distances 2, 3, and 4, classification probabilities obtained for the classifiers (n = 32) trained on nonsymbolic and symbolic number neurons were almost identical and significantly higher for symbolic than for nonsymbolic number ($p < 0.01$; t test). This indicates a sharper transition from the preferred to all nonpreferred numbers and thus greater selectivity in neurons tuned to symbolic number. When applied to the entire set of single units regardless of numerosity selectivity (585 units), this analysis yielded qualitatively similar results (Figure S4).

In addition, we analyzed the coding capacity and dynamics of the population of number-selective neurons by performing a multi-dimensional state-space analysis (see Supplemental Information) for nonsymbolic and symbolic numbers separately. At each point in time, the activity of *n* recorded neurons is defined by a point in *n*-dimensional space, with each dimension representing the activity of a single neuron. This results in trajectories that are traversed for different neuronal states, i.e., the five different numerical values in the nonsymbolic (Figure 6A, left) and symbolic format (Figure 6A, right). These trajectories reflect the instantaneous firing rates of the respective neuronal population as they evolve over time. To evaluate the temporal evolution of population numerical tuning in each format, we measured Euclidian distances between trial trajectories in the whole

population space corresponding to the activity to the five numerical values. In the nonsymbolic format, the trajectory distances systematically increased with numerical distance ($p < 0.001$; permutation test for all trajectories; see Supplemental Information), starting shortly after onset of operand 1 until the end of the memory delay 1. The distances between the population trajectories confirm the findings based on single selective neurons: the closer two numerosities were in the numerical continuum, the more similar were the corresponding patterns of population activity and vice versa (Figure 6B, left). This argues for a numerical distance effect in the population data. In the symbolic format, the trajectory distances were much less pronounced but likewise tended to increase with numerical distance ($p < 0.001$ for 1 versus 4 in a permutation test), reflecting the remnants of a distance effect (Figure 6B, right). A comparison of the trajectory distances also suggests that MTL neurons responded longer lasting to the nonsymbolic format and throughout the working memory period (i.e., delay 1). In contrast, the responses to the symbolic format were more confined to the sample phase of operand 1. Again, this analysis yielded similar results when performed for the whole population of single units (Figure S5).

Encoding of Number in Later Task Phases

After analysis of the responses to the operand 1, we also examined selectivity to the numerical value of operand 2 separately for nonsymbolic and symbolic number format. For the nonsymbolic format, 7.7% (45/585) of the tested neurons showed activity that varied exclusively with the number of operand 2 items during operand 2 presentation, irrespective of the dot array layout (5-factor sliding-window ANOVA with the factors numerical value of operand 1 [1–5], numerical value of operand 2 [0–5], protocol [standard and control], "mathematical rule" [addition and subtraction], and "rule cue" [word and symbol]; $\alpha = 0.01$). Twenty-two of the units selective to nonsymbolic operand 1 ($n = 92$) were also tuned to nonsymbolic operand 2; of those, 9 cells had the same preferred number. Given that 20% of the selective units are expected to share the preferred number by chance (5 number values), this proportion of 9 cells was significantly higher ($p < 0.05$ in binomial test). The finding that cells that responded both to operand 1 and operand 2 tended to show the same preferred numerosity was also confirmed by a correlation analysis (Pearson's $r = 0.64$; $p = 0.0013$; Figure S6). For the symbolic format, only a chance proportion of 1.5% (9/585) responded exclusively to the numerical value of the operand 2 during the presentation of the operand 2.

The responses of a single neuron throughout the whole trial are shown in Figure S7. This neuron was significantly tuned to numerosity 5 of operand 1 during the operand 1 phase and of operand 2 during the operand 2 phase (Figure S7, upper histograms). This neuron also showed strong responses to the numerical values of the operand 2 during the symbolic format (Figure S7, lower histograms); however, it was also selective to the numeral protocol and thus not counted as an exclusively numeral-selective cell. Overall, the highest proportion of neurons selective to the nonsymbolic numerical value of operand 2 in the MTL was found in the parahippocampal cortex (20%), followed by the hippocampus (6%; Figure S8).

Next, we analyzed selectivity to number in the delay 2 phase, again separately for nonsymbolic and symbolic number format. In the delay 2 phase, all the information necessary to solve the calculation is available to the subjects. The delay 2 phase may therefore be regarded as the calculation result phase. For statistical analysis, we applied a sliding-window 6-factor ANOVA (with the same factors as above, plus main factor numerical value corresponding to the result of the calculation [0–9]; $\alpha = 0.01$). Neither for the nonsymbolic nor for the symbolic format was the proportion of neurons selective to the calculation result higher than expected by chance (Figure S8).

Representation of Calculation Rules

Finally, we explored whether MTL neurons also encoded the calculation rules (addition and subtraction) in an abstract manner, independent from the rule notation (word or calculation symbol as rule cues). Cells selective to nonsymbolic numerical rules have been found in monkey cortex (Vallentin et al., 2012; Eiselt and Nieder, 2013). We determined calculation rule-selective units by applying a sliding-window 4-factor ANOVA (with the factors mathematical rule [addition and subtraction], rule cue [word and symbol], numerical value of operand 1 [1–5], and format [symbolic and nonsymbolic]; $\alpha = 0.01$) during the calculation rule phase and the rule delay phase. Figure S9 displays two rule-selective neurons. The neuron in Figure S9A showed a selective increase whenever an addition was required (reddish discharges), whereas the neuron in Figure S9B selectively enhanced discharges whenever a subtraction was cued (blueish colors). These rule-selective response increases were abstract and independent from the notation of the rule cue (word or symbol). In total, we found only a small proportion of 2% of abstract calculation rule cells, but this fraction was significantly larger than expected by chance (Figure S10). In addition, a significant fraction of 3% of the cells encoded the rule cue (calculation word or symbol) during the calculation rule phase (Figure S10).

DISCUSSION

Using single-cell recordings in subjects performing a calculation task, we have shown that single neurons in the MTL of humans are tuned to numerical values in nonsymbolic dot displays and symbolic numerals. The data about nonsymbolic number coding from humans can now be compared to those of nonhuman primates. In addition, our MTL recordings show how the capacity to represent symbolic number is represented in this part of our brain. This capacity to link number to visual signs has precursors in nonhuman primates (Diester and Nieder, 2010; Livingstone et al., 2014), but ultimately the symbolic number system is uniquely human (Nieder, 2009).

Functional imaging studies in humans found that areas of the MTL—among many other functions outside of the number domain—participate in learning arithmetic (De Smedt et al., 2011; Supekar et al., 2013; Qin et al., 2014; Menon, 2016). Using single-cell recordings in human subjects, we show that MTL neurons encode the numerical values in both nonsymbolic and symbolic number. With 29% and 6% of all neurons being selective to nonsymbolic and symbolic number, respectively, the parahippocampal cortex (PHC) shows the highest proportions of number

neurons among the four tested MTL areas. The PHC is part of a large network that connects regions of the temporal, parietal, and frontal cortices and has been associated with many cognitive processes (Aminoff et al., 2013), such as selectivity to pictures (Kreiman et al., 2000), responses guided by familiarity (Rutishauser et al., 2006), responses to spatial factors (Jacobs et al., 2013), and responses to mirror actions (Mukamel et al., 2010). Most likely, representations about numerical quantity do not originate within the PHC (or other areas of the MTL) but are provided via direct anatomical connections to the parieto-frontal core number system (Goldman-Rakic et al., 1984). Interestingly, the PHC has prominent connections with polymodal association areas, including the parietal lobule (Suzuki, 2009). This connection with the parietal lobule, an integral part of the core number network (Piazza et al., 2004, 2007; Arsalidou and Taylor, 2011) in which numerosity, but not number symbols, are mapped topographically (Harvey et al., 2013) is likely to provide the PHC with semantic information about numerical magnitude.

We have discovered two largely segregated populations of tuned number neurons in the human MTL that process either nonsymbolic or symbolic numerical quantity. The representation of nonsymbolic and symbolic number information by two distinct populations of tuned number neurons may either be inherited from the core number system or a special feature of the human MTL. Neurons in the prefrontal cortex of monkeys have been shown to respond abstractly by integrating visual and auditory numerosity (Nieder, 2012). Of course, number neurons in nonhuman primates operate strictly within the nonsymbolic format, but in monkeys trained to associate visual shapes with varying numbers of items, the responses of prefrontal neurons to the visual shapes reflected the associated numerical value in a behaviorally relevant way (Diester and Nieder, 2007).

Irrespective of its neurophysiological realization, format dependency does not pose a conceptual problem to number coding. In the human functional imaging literature, it is debated to what extent neural representations of number even in the human intraparietal sulcus (IPS) are format independent (Piazza et al., 2007; Eger et al., 2009; Jacob and Nieder, 2009b; Damarla et al., 2016) or format dependent (Cohen Kadosh et al., 2007; Holloway et al., 2010). There is not even consensus with regard to the degree of abstractness of numerical representations (reviewed in Cohen Kadosh and Walsh, 2009). Of course, these findings derived from blood-oxygen-level-dependent signals might also be explained by functionally segregated circuits that overlap at the macroscopic voxel scale. Future single-cell recordings in human subjects, in particular in the parietal and frontal association cortices, may help to resolve the question of abstract or segregated number neurons. They could also provide insights into the coding of larger numbers, the empty set, and the special number zero (Merten and Nieder, 2012; Ramirez-Cardenas et al., 2016).

Our study also helps to answer the question of the neuronal code for number. Two competing hypotheses have been proposed. Numbers could either be encoded by a "summation code," as evidenced by monotonic discharges as a function of quantity (Roitman et al., 2007), or by a "labeled-line code" as witnessed by numerosity-selective neurons tuned to preferred numerosities. In agreement with influential computational models of number processing (Dehaene and Changeux, 1993; Verguts and Fias, 2004), the number neurons we found in the human MTL were tuned to their individual preferred numerical value. A general concern of data from patients with a history of epileptic seizures is of course that the functional properties of MTL neurons may have affected during the course of the disease. Moreover, eye movement that was not measured during human recordings might have influenced the neurons' response properties. However, such factors are unlikely responsible for our results, because the same code that we observed in MTL neurons has been found multiple times in single-cell recordings of fixating monkeys, both in trained (Nieder et al., 2002, 2006; Sawamura et al., 2002; Nieder and Miller, 2004; Nieder, 2012) and numerically naive subjects (Viswanathan and Nieder, 2013) and even in corvid birds (Ditz and Nieder, 2015). This coding similarity suggests that our findings in the MTL are representative also for the healthy human brain. In addition, it indicates that number coding in humans and other animals is best captured by a labeled-line code. Of course, because number neurons only represent a very restricted part of the number line, only populations of number neurons, each tuned to different values, can represent the entire "mental number line."

In order to link number neurons to numerical behavior, neuronal responses need to explain number judgments (Nieder and Miller, 2003; Pinel et al., 2004). The direct comparison of responses in error trials versus correct trials, an analysis regularly done in nonhuman primates, would have been informative, but the human subjects hardly made any error and thus precluded the evaluation of error trials. However, as a basic requirement supporting the link between neurons and behavior, we show that nonsymbolic and symbolic numerical values can be reliably decoded from MTL neurons (Ramirez-Cardenas et al., 2016). This holds true for the populations of selective number neurons but also for the entire population of recorded neurons and irrespective of response selectivity. In addition, the neuronal activity can also explain the numerical distance effect, the finding that numerically distant numbers can be better discriminated. Behavioral studies and neural modeling show that the distance effect is substantial for the comparison of nonsymbolic numerosities but minute for judgments of exact number symbols (Buckley and Gillman, 1974; Verguts and Fias, 2004). In agreement with this, the accuracy of number discrimination based on the neuronal discharges exhibited large distance effects for the populations of broadly tuned numerosity-selective neurons but small distance effects for sharply tuned numeral-selective neurons. This finding provides further evidence for these neurons as the physiological correlate of number representations.

The distance effect for number symbols is thought to be inherited from more basic nonsymbolic number representations (Moyer and Landauer, 1967; Buckley and Gillman, 1974; Piazza et al., 2007). Its presence in human number neurons therefore supports the hypothesis that high-level human numerical abilities are rooted in biologically determined mechanisms. It suggests that number symbols acquire their numerical meaning by becoming linked to evolutionarily conserved set size representations during cognitive development (Halberda et al., 2008; Szkudlarek and Brannon, 2017). Symbolic number cognition thus appears to be grounded in neuronal circuits devoted to deriving

precise numerical values from approximate numerosity representations (Dehaene and Cohen, 2007).

STAR★METHODS

Detailed methods are provided in the online version of this paper and include the following:

- KEY RESOURCES TABLE
- CONTACT FOR REAGENT AND RESOURCE SHARING
- EXPERIMENTAL MODEL AND SUBJECT DETAILS
- METHOD DETAILS
  - Neurophysiological Recording
  - Stimuli
  - Experimental Task
- QUANTIFICATION AND STATISTICAL ANALYSIS
  - Sliding-Window 2-Factor Analysis of Variance (ANOVA)
  - Tuning Properties
  - Multi-Class Support Vector Machine (SVM) Classification
  - Population State-Space Analysis
  - Other Task Phases
- DATA AND SOFTWARE AVAILABILITY

SUPPLEMENTAL INFORMATION

Supplemental Information includes ten figures and one table and can be found with this article online at https://doi.org/10.1016/j.neuron.2018.08.036.

ACKNOWLEDGMENTS

We thank all patients for their participation. This research was supported by the Volkswagen Foundation, Germany, and the German Research Council (MO930/4-1 and SFB1089).

AUTHOR CONTRIBUTIONS

A.N. and F.M. designed the study; C.E.E. and F.M. recruited patients; J.B. and F.M. implanted the electrodes; E.F.K. and F.M. collected the data; E.F.K. analyzed the data with contributions from A.N. and F.M.; and A.N., E.F.K., and F.M. wrote the paper. All authors discussed the results and commented on the manuscript.

DECLARATION OF INTERESTS

The authors declare no competing interests.

Received: March 9, 2018
Revised: June 19, 2018
Accepted: August 24, 2018
Published: September 20, 2018

REFERENCES

Aminoff, E.M., Kveraga, K., and Bar, M. (2013). The role of the parahippocampal cortex in cognition. Trends Cogn. Sci. *17*, 379–390.

Arsalidou, M., and Taylor, M.J. (2011). Is 2+2=4? Meta-analyses of brain areas needed for numbers and calculations. Neuroimage *54*, 2382–2393.

Brannon, E.M., and Terrace, H.S. (1998). Ordering of the numerosities 1 to 9 by monkeys. Science *282*, 746–749.

Buckley, P.B., and Gillman, C.B. (1974). Comparisons of digits and dot patterns. J. Exp. Psychol. *103*, 1131–1136.

Chang, C.-C., and Lin, C.-J. (2011). LIBSVM: a library for support vector machines. ACM Trans. Intell. Syst. Technol. *2*, 27.

Cohen Kadosh, R., and Walsh, V. (2009). Numerical representation in the parietal lobes: abstract or not abstract? Behav. Brain Sci. *32*, 313–328, discussion 328–373.

Cohen Kadosh, R., Cohen Kadosh, K., Kaas, A., Henik, A., and Goebel, R. (2007). Notation-dependent and -independent representations of numbers in the parietal lobes. Neuron *53*, 307–314.

Daitch, A.L., Foster, B.L., Schrouff, J., Rangarajan, V., Kaşikçi, I., Gattas, S., and Parvizi, J. (2016). Mapping human temporal and parietal neuronal population activity and functional coupling during mathematical cognition. Proc. Natl. Acad. Sci. USA *113*, E7277–E7286.

Damarla, S.R., Cherkassky, V.L., and Just, M.A. (2016). Modality-independent representations of small quantities based on brain activation patterns. Hum. Brain Mapp. *37*, 1296–1307.

De Smedt, B., Holloway, I.D., and Ansari, D. (2011). Effects of problem size and arithmetic operation on brain activation during calculation in children with varying levels of arithmetical fluency. Neuroimage *57*, 771–781.

Dehaene, S. (1997). The Number Sense (Oxford: Oxford Univ. Press).

Dehaene, S., and Changeux, J.P. (1993). Development of elementary numerical abilities: a neuronal model. J. Cogn. Neurosci. *5*, 390–407.

Dehaene, S., and Cohen, L. (2007). Cultural recycling of cortical maps. Neuron *56*, 384–398.

Diester, I., and Nieder, A. (2007). Semantic associations between signs and numerical categories in the prefrontal cortex. PLoS Biol. *5*, e294.

Diester, I., and Nieder, A. (2010). Numerical values leave a semantic imprint on associated signs in monkeys. J. Cogn. Neurosci. *22*, 174–183.

Ditz, H.M., and Nieder, A. (2015). Neurons selective to the number of visual items in the corvid songbird endbrain. Proc. Natl. Acad. Sci. USA *112*, 7827–7832.

Eger, E., Michel, V., Thirion, B., Amadon, A., Dehaene, S., and Kleinschmidt, A. (2009). Deciphering cortical number coding from human brain activity patterns. Curr. Biol. *19*, 1608–1615.

Eiselt, A.K., and Nieder, A. (2013). Representation of abstract quantitative rules applied to spatial and numerical magnitudes in primate prefrontal cortex. J. Neurosci. *33*, 7526–7534.

Fried, I., MacDonald, K.A., and Wilson, C.L. (1997). Single neuron activity in human hippocampus and amygdala during recognition of faces and objects. Neuron *18*, 753–765.

Gilmore, C.K., McCarthy, S.E., and Spelke, E.S. (2010). Non-symbolic arithmetic abilities and mathematics achievement in the first year of formal schooling. Cognition *115*, 394–406.

Goldman-Rakic, P.S., Selemon, L.D., and Schwartz, M.L. (1984). Dual pathways connecting the dorsolateral prefrontal cortex with the hippocampal formation and parahippocampal cortex in the rhesus monkey. Neuroscience *12*, 719–743.

Gordon, P. (2004). Numerical cognition without words: evidence from Amazonia. Science *306*, 496–499.

Halberda, J., Mazzocco, M.M.M., and Feigenson, L. (2008). Individual differences in non-verbal number acuity correlate with maths achievement. Nature *455*, 665–668.

Harvey, B.M., Klein, B.P., Petridou, N., and Dumoulin, S.O. (2013). Topographic representation of numerosity in the human parietal cortex. Science *341*, 1123–1126.

Holloway, I.D., Price, G.R., and Ansari, D. (2010). Common and segregated neural pathways for the processing of symbolic and nonsymbolic numerical magnitude: an fMRI study. Neuroimage *49*, 1006–1017.

Jacob, S.N., and Nieder, A. (2009a). Tuning to non-symbolic proportions in the human frontoparietal cortex. Eur. J. Neurosci. *30*, 1432–1442.

Jacob, S.N., and Nieder, A. (2009b). Notation-independent representation of fractions in the human parietal cortex. J. Neurosci. *29*, 4652–4657.

Jacobs, J., Weidemann, C.T., Miller, J.F., Solway, A., Burke, J.F., Wei, X.X., Suthana, N., Sperling, M.R., Sharan, A.D., Fried, I., and Kahana, M.J. (2013). Direct recordings of grid-like neuronal activity in human spatial navigation. Nat. Neurosci. *16*, 1188–1190.

Kreiman, G., Koch, C., and Fried, I. (2000). Category-specific visual responses of single neurons in the human medial temporal lobe. Nat. Neurosci. *3*, 946–953.

Livingstone, M.S., Pettine, W.W., Srihasam, K., Moore, B., Morocz, I.A., and Lee, D. (2014). Symbol addition by monkeys provides evidence for normalized quantity coding. Proc. Natl. Acad. Sci. USA *111*, 6822–6827.

Maris, E., and Oostenveld, R. (2007). Nonparametric statistical testing of EEG- and MEG-data. J. Neurosci. Methods *164*, 177–190.

Menon, V. (2016). Memory and cognitive control circuits in mathematical cognition and learning. Prog. Brain Res. *227*, 159–186.

Merten, K., and Nieder, A. (2009). Compressed scaling of abstract numerosity representations in adult humans and monkeys. J. Cogn. Neurosci. *21*, 333–346.

Merten, K., and Nieder, A. (2012). Active encoding of decisions about stimulus absence in primate prefrontal cortex neurons. Proc. Natl. Acad. Sci. USA *109*, 6289–6294.

Mormann, F., Dubois, J., Kornblith, S., Milosavljevic, M., Cerf, M., Ison, M., Tsuchiya, N., Kraskov, A., Quiroga, R.Q., Adolphs, R., et al. (2011). A category-specific response to animals in the right human amygdala. Nat. Neurosci. *14*, 1247–1249.

Moyer, R.S., and Landauer, T.K. (1967). Time required for judgements of numerical inequality. Nature *215*, 1519–1520.

Mukamel, R., Ekstrom, A.D., Kaplan, J., Iacoboni, M., and Fried, I. (2010). Single-neuron responses in humans during execution and observation of actions. Curr. Biol. *20*, 750–756.

Nieder, A. (2009). Prefrontal cortex and the evolution of symbolic reference. Curr. Opin. Neurobiol. *19*, 99–108.

Nieder, A. (2012). Supramodal numerosity selectivity of neurons in primate prefrontal and posterior parietal cortices. Proc. Natl. Acad. Sci. USA *109*, 11860–11865.

Nieder, A. (2016). The neuronal code for number. Nat. Rev. Neurosci. *17*, 366–382.

Nieder, A., and Merten, K. (2007). A labeled-line code for small and large numerosities in the monkey prefrontal cortex. J. Neurosci. *27*, 5986–5993.

Nieder, A., and Miller, E.K. (2003). Coding of cognitive magnitude: compressed scaling of numerical information in the primate prefrontal cortex. Neuron *37*, 149–157.

Nieder, A., and Miller, E.K. (2004). A parieto-frontal network for visual numerical information in the monkey. Proc. Natl. Acad. Sci. USA *101*, 7457–7462.

Nieder, A., Freedman, D.J., and Miller, E.K. (2002). Representation of the quantity of visual items in the primate prefrontal cortex. Science *297*, 1708–1711.

Nieder, A., Diester, I., and Tudusciuc, O. (2006). Temporal and spatial enumeration processes in the primate parietal cortex. Science *313*, 1431–1435.

Niediek, J., Boström, J., Elger, C.E., and Mormann, F. (2016). Reliable analysis of single-unit recordings from the human brain under noisy conditions: tracking neurons over hours. PLoS ONE *11*, e0166598.

Piazza, M., Izard, V., Pinel, P., Le Bihan, D., and Dehaene, S. (2004). Tuning curves for approximate numerosity in the human intraparietal sulcus. Neuron *44*, 547–555.

Piazza, M., Pinel, P., Le Bihan, D., and Dehaene, S. (2007). A magnitude code common to numerosities and number symbols in human intraparietal cortex. Neuron *53*, 293–305.

Pica, P., Lemer, C., Izard, V., and Dehaene, S. (2004). Exact and approximate arithmetic in an Amazonian indigene group. Science *306*, 499–503.

Pinel, P., Piazza, M., Le Bihan, D., and Dehaene, S. (2004). Distributed and overlapping cerebral representations of number, size, and luminance during comparative judgments. Neuron *41*, 983–993.

Qin, S., Cho, S., Chen, T., Rosenberg-Lee, M., Geary, D.C., and Menon, V. (2014). Hippocampal-neocortical functional reorganization underlies children's cognitive development. Nat. Neurosci. *17*, 1263–1269.

Quiroga, R.Q., Reddy, L., Kreiman, G., Koch, C., and Fried, I. (2005). Invariant visual representation by single neurons in the human brain. Nature *435*, 1102–1107.

Ramirez-Cardenas, A., Moskaleva, M., and Nieder, A. (2016). Neuronal representation of numerosity zero in the primate parieto-frontal number network. Curr. Biol. *26*, 1285–1294.

Reber, T.P., Faber, J., Niediek, J., Boström, J., Elger, C.E., and Mormann, F. (2017). Single-neuron correlates of conscious perception in the human medial temporal lobe. Curr. Biol. *27*, 2991–2998.e2.

Roitman, J.D., Brannon, E.M., and Platt, M.L. (2007). Monotonic coding of numerosity in macaque lateral intraparietal area. PLoS Biol. *5*, e208.

Rutishauser, U., Mamelak, A.N., and Schuman, E.M. (2006). Single-trial learning of novel stimuli by individual neurons of the human hippocampus-amygdala complex. Neuron *49*, 805–813.

Sawamura, H., Shima, K., and Tanji, J. (2002). Numerical representation for action in the parietal cortex of the monkey. Nature *415*, 918–922.

Scarf, D., Hayne, H., and Colombo, M. (2011). Pigeons on par with primates in numerical competence. Science *334*, 1664.

Starr, A., Libertus, M.E., and Brannon, E.M. (2013). Number sense in infancy predicts mathematical abilities in childhood. Proc. Natl. Acad. Sci. USA *110*, 18116–18120.

Supekar, K., Swigart, A.G., Tenison, C., Jolles, D.D., Rosenberg-Lee, M., Fuchs, L., and Menon, V. (2013). Neural predictors of individual differences in response to math tutoring in primary-grade school children. Proc. Natl. Acad. Sci. USA *110*, 8230–8235.

Suzuki, W.A. (2009). Comparative analysis of the cortical afferents, intrinsic projections and interconnections of the parahippocampal region in monkeys and rats. In The Cognitive Neurosciences IV, M.S. Gazzaniga, ed. (Cambridge: MIT Press), pp. 659–674.

Szkudlarek, E., and Brannon, E.M. (2017). Does the approximate number system serve as a foundation for symbolic mathematics? Lang. Learn. Dev. *13*, 171–190.

Vallentin, D., Bongard, S., and Nieder, A. (2012). Numerical rule coding in the prefrontal, premotor, and posterior parietal cortices of macaques. J. Neurosci. *32*, 6621–6630.

Verguts, T., and Fias, W. (2004). Representation of number in animals and humans: a neural model. J. Cogn. Neurosci. *16*, 1493–1504.

Viswanathan, P., and Nieder, A. (2013). Neuronal correlates of a visual "sense of number" in primate parietal and prefrontal cortices. Proc. Natl. Acad. Sci. USA *110*, 11187–11192.

Wynn, K. (1992). Addition and subtraction by human infants. Nature *358*, 749–750.

Xu, F., and Spelke, E.S. (2000). Large number discrimination in 6-month-old infants. Cognition *74*, B1–B11.

Yu, B.M., Cunningham, J.P., Santhanam, G., Ryu, S.I., Shenoy, K.V., and Sahani, M. (2009). Gaussian-process factor analysis for low-dimensional single-trial analysis of neural population activity. J. Neurophysiol. *102*, 614–635.

STAR★METHODS

KEY RESOURCES TABLE

REAGENT or RESOURCE	SOURCE	IDENTIFIER
Software and Algorithms		
Cheetah software	Neuralynx Inc.	https://neuralynx.com/software/cheetah
Combinato spike sorting software	Niediek et al. (2016)	https://github.com/jniediek/combinato
MATLAB R2017a	MathWorks	https://de.mathworks.com/
Psychtoolbox		http://psychtoolbox.org/
LIBSVM	Chang and Lin (2011)	https://www.csie.ntu.edu.tw/~cjlin/libsvm/
DataHigh	Yu et al. (2009)	https://users.ece.cmu.edu/~byronyu/software/DataHigh/datahigh.html
Other		
Behnke-Fried depth electrodes	AD-TECH Medical Instrument Corp.	https://adtechmedical.com/depth-electrodes
ATLAS neurophysiology system	Neuralynx Inc.	https://neuralynx.com/news/techtips/atlas-neurophysiology-system-for-cogneuro-applications

CONTACT FOR REAGENT AND RESOURCE SHARING

Further information and requests for resources should be directed to and will be fulfilled by Florian Mormann (florian.mormann@ukbonn.de).

EXPERIMENTAL MODEL AND SUBJECT DETAILS

Nine human subjects (4 male, all right-handed, mean age 43.3 years) undergoing treatment for pharmacologically intractable epilepsy participated in the study. Informed written consent was obtained from each patient. All studies conformed to the guidelines of the Medical Institutional Review Board at the University of Bonn, Germany. On the level of single neurons no sex- or gender-specific differences are to be expected; thus, the influence of sex and gender identity was not analyzed further.

METHOD DETAILS

Neurophysiological Recording

All subjects were implanted bilaterally with chronic intracerebral depth electrodes in the medial temporal lobe (MTL) to localize the epileptic focus for possible clinical resection. The exact electrode numbers and locations varied across subjects and were based exclusively on clinical criteria. Neuronal signals were recorded using 9–10 clinical Behnke-Fried depth electrodes (AD-TECH Medical Instrument Corp., Racine, WI). Each electrode contained a bundle of nine platinum-iridium micro-electrodes protruding from its tip; eight high-impedance active recording channels, and one low-impedance reference electrode. Differential neuronal signals (recording range ± 3200 μV) were filtered (bandwidth 0.1–9,000 Hz), amplified and digitized (sampling rate 32.7 kHz) using a 256-channel ATLAS neurophysiology system (Neuralynx Inc., Bozeman, MT). Behavioral data were synchronized with the recorded spikes via 8-bit timestamps using the Cheetah software (Neuralynx Inc., Bozeman, MT).

After band-pass filtering the signals (bandwidth 300–3,000 Hz), spikes were detected and pre-sorted automatically using the Combinato software (Niediek et al., 2016). Manual verification and classification as artifact, multi or single unit was based on spike shape and its variance, inter-spike interval distribution per cluster and the presence of a plausible refractory period. Only units that responded with an average firing rate of > 1 Hz during operand 1 and delay 1 phase for either format were included in the analyses. Across 16 recording sessions from all nine patients, a total of 836 units (585 single and 251 multi units) were identified in the amygdala (AMY; 153 single and 63 multi units), parahippocampal cortex (PHC; 126 single and 61 multi units), entorhinal cortex (EC; 107 single and 54 multi units) and hippocampus (HIPP; 199 single and 73 multi units) according to these criteria (see Table S1); 333 units with firing rates < 1 Hz were excluded. Only single units were subjected to further analyses.

Stimuli

All stimuli were presented within a filled gray circle (diameter 6° of visual angle) on a black background. During fixation and delay phases, a white fixation spot was presented in the center of the gray area. It disappeared during stimulus presentation to avoid

confusion with nonsymbolic stimuli and to distinguish it clearly from the nonsymbolic zero-stimulus that was included for control purposes as a potential operand 2-stimulus (see *Experimental Task*).

Number stimuli of operand 1 ranged from 1 to 5, and were either black 'symbolic' Arabic digits at a randomized location ('numerals'), or 'nonsymbolic' arrays of black dots of pseudo-randomly varied sizes and at randomized locations where the number of dots corresponded to the respective numerical value ('numerosities'). Number stimuli of operand 2 ranged from 0 to 5, and were the same as for operand 1. For the nonsymbolic 'zero'-stimulus the empty gray circle without fixation spot was presented.

Both nonsymbolic and symbolic number formats were shown in standard and control displays, or 'protocols' (Figure 1B). This was done in order to control for low-level visual features. The standard nonsymbolic numerosity displays consisted of randomly placed dots of varying sizes (diameter 0.3° to 0.8° of visual angle), whereas in the control displays the overall surface area and density of the dots across numerosities was equated. For the Arabic numerals, different font types were used as standard (Helvetica, 34 pt) and control (DS-Digital, 34 pt) displays. A session consisted of 50% nonsymbolic and 50% symbolic number formats. Within each format, standard and control protocols were shown with equal probability of 50%.

Two different mathematical rules, i.e., addition and subtraction, were applied (Figure 1C). To dissociate neuronal activity related purely to physical properties of the operator from the rule that it signifies, two distinct cues, i.e., the mathematical sign (+ or –) or a verbal analog ('und' [add] and 'weniger' [subtract]), were used for each rule (all Helvetica, 34 pt, and presented in the center).

Experimental Task

During experimental sessions, subjects sat in bed and performed the task on a touch-screen laptop (display diagonal 11.7 in; resolution 1366x768 px) on which stimuli were presented at a distance of approximately 50 cm. To exclude any bias, the subjects were not informed about the purpose or hypotheses of the experiment.

Subjects performed two calculation tasks that required them to calculate the result of a simple arithmetic problem (Figure 1A). Each trial started with a 500 ms fixation phase. Then, stimuli were presented successively in the order operand 1 – operator – operand 2 for 500 ms each, followed each by 800 ms delay phases. Afterward, a number pad showing the Arabic numerals 0 to 9 was presented on the screen and subjects were instructed to touch the number matching the result of the calculation in a self-paced manner. After a 500 ms feedback display ('richtig' [correct] or 'falsch' [false]) the next trial was started automatically.

We varied five factors in this task: Format (symbolic/ nonsymbolic), numerical value (1–5), and protocol (standard/ control) for the operand 1-stimulus, resulting in 20 different 'number' conditions, as well as mathematical rule (addition/ subtraction) and rule cue (symbol/ word), resulting in four 'operator' conditions. Operand 2 was always of the same format and protocol as operand 1, but with random numerical value 0–5, albeit guaranteeing calculation results between 0 and 9.

Each session comprised a total of 320 trials, plus 10 rehearsal trials at the beginning to familiarize subjects with the task that were excluded from further analysis. A session was divided into four blocks of 80 trials each, comprising each of the 80 different conditions in pseudo-random order, to allow for short self-paced breaks in between. Thus, every number condition (i.e., combination of number, format and protocol) was presented 16 times, while every operator condition (i.e., combination of rule and rule cue) occurred 80 times.

QUANTIFICATION AND STATISTICAL ANALYSIS

Only single units (n = 585) were included in the following analyses. We focused on the operand 1 and delay 1 phases because these were the only periods during which pure number information was being processed. Given that the rule to be applied was not yet known, interference of calculation processes or motor response preparation could be excluded. Thus, all analyses were conducted for the time window 0–1850 ms (fixation onset to delay 1 offset). All subjects performed the task with high proficiency (98.5% ± 0.6%, range 90.3%–99.8%). Therefore, we did not exclude the negligible number of error trials from the analyses.

Sliding-Window 2-Factor Analysis of Variance (ANOVA)

Due to the incomparability of the protocol conditions for the different formats, the following procedure was carried out separately for trials of each format. For each unit, spike trains were smoothed trial-wise (Gaussian kernel, $\sigma = 150$ ms) within the analysis window. At every 10-ms-step, a 2-factor ANOVA was performed on the instantaneous firing rates for the factors 'numerical value' (1–5) and 'protocol' (standard/ control) resulting in a temporal sequence of *F*-values for main and interaction effects. To control for multiple comparisons, a cluster permutation test (Maris and Oostenveld, 2007) was performed to identify temporal clusters that encoded number information significantly. Briefly, all *F*-values within a cluster, i.e., an interval with only significant *p*-values ($p_{clus} < 0.01$) for the respective effect, were summed up. Calculating multiple 2-factor ANOVAs and summing up significant *F*-values was repeated with randomly shuffled trial labels ($n_{perm} = 100$). A temporal cluster of the true data was then considered significant only if the percentile rank of the summed *F*-values of the true data was significant across the distribution of summed *F*-values obtained for the shuffled data ($p_{rank} < 1\%$, corresponding to a nominal size of the statistical test of $\alpha = 0.01$). In the following, we refer to such a significant cluster as NUM-interval. A unit was counted as exclusively number-selective ('number-unit') if a significant cluster was observed between 500–1600 ms (operand 1 onset to 200 ms before delay 1 offset) for the factor 'numerical value' and there were no overlapping significant clusters for the factor 'protocol' or the interaction (see Figure S1). As a control, we determined the proportion of significant NUM-intervals for the shuffled data (585 single units x 100 permutations, resulting in 58,500 tests; same procedure as for the true

data) in order to estimate the probability of false positives, i.e., the probability that a unit was classified as number-selective by chance. For both formats, we found that 1% of these tests (nonsymbolic 493/58,500, symbolic 513/58,500) resulted in a statistically significant result, or false positive, confirming the empirical size of the statistical test to also be at $\alpha \approx 0.01$. The probability that neuronal selectivity occurs by chance was therefore 1%. Using a binomial test with $p_{chance} = \alpha = 0.01$, we can thus confirm that the observed proportion of number-selective neurons cannot be explained by chance occurrences both for nonsymbolic (92/585; $p_{binomial}$ = 1.18e-77) and symbolic (16/585; $p_{binomial}$ = 3.58e-4) number-selective neurons.

To compare the general response behavior of number-units and non-selective cells, we determined the maximum firing rate per number condition for each format and cell by averaging the spike rates within the significant NUM-interval for the number-units or across the entire operand 1 and delay 1 phase (500–1800 ms) for the non-selective units (nonsymbolic format: 92 numerosity-cells, 493 non-selective cells; symbolic format: 16 numeral-cells, 569 non-selective cells). Distributions were then compared using a Mann-Whitney-U-test (see Figure S2). The correlation between nonsymbolic and symbolic number-representations was evaluated for the sub-populations of numerosity-selective neurons (n = 92), numeral-selective neurons (n = 16) and neurons responsive to both formats (n = 6). For each unit of a sub-population, we calculated the preferred number for the significant format by averaging the spike rates during the respective NUM-interval, and the preferred number for the non-significant format by averaging the spike rates across the entire operand 1 and delay 1 phase (500–1800 ms). We then quantified the relationship by calculating Pearson's linear correlation coefficient (see Figure S3).

The sub-populations of nonsymbolic and symbolic number-units obtained with the sliding-window 2-factor ANOVA showed little (although significant) overlap. Therefore, the following population analyses were performed separately for the sub-population of nonsymbolic number-units (92 units) considering nonsymbolic trials only, and the sub-population of neurons preferring symbolic stimuli (16 units) using symbolic trials only. For control purposes, population analyses were also performed for the whole population of single units (585 units; see Figures S4 and S5).

Tuning Properties

For each number-unit, individual tuning curves were obtained by averaging the responses to different numerical values across trials, during the time window of significant number-clusters (NUM-intervals). In cases where we identified multiple NUM-intervals within the same unit, tuning curves were calculated separately for each of these intervals (3/5 nonsymbolic number-cells with multiple NUM-intervals preferred different numerosities). They were then normalized by setting the maximum response to 100% and the minimum response to 0%. The preferred numerical value was determined as the number which elicited the strongest average response. A cross-validation analysis was performed to estimate the robustness and reliability of the preferred number assessment (Nieder and Merten, 2007). We split the data into two halves by randomly assigning the trials to either of the two sets and calculated the preferred number for each dataset. This was done for the entire population of number-units and the relationship between preferred numbers quantified by calculating Pearson's linear correlation coefficient. If both datasets resulted in identical preferred numbers, the correlation coefficient was 1. The correlation analysis was performed 100 times for different random partitions of the data, and the average correlation coefficient was calculated.

Population neural filter functions were then calculated by averaging across the sub-populations of units preferring the same numerical value. The activity of each number-unit was considered as a function of distance from its preferred number. Differences between all pairs of adjacent numerical distances were separately quantified using Wilcoxon signed-rank tests. Moreover, for each numerical distance we tested whether the obtained response differed significantly from a response pattern to be expected in case of random tuning (obtained by repeating the analysis with shuffled labels) using a permutation test (n_{perm} = 1000).

Multi-Class Support Vector Machine (SVM) Classification

For each unit, spike trains were trial-wise smoothed (Gaussian kernel, σ = 50 ms, window size 300 ms) within the analysis window. For temporal cross-training classification, a multi-class SVM classifier (Chang and Lin, 2011) was trained on the instantaneous firing rates at a certain time point, and then tested on firing rates at different time points (sampling interval 10 ms). We used a linear SVM-kernel with default parameter settings and applied 'one-versus-one' classification to distinguish our five classes. For the 32 trials per number and format (symbolic versus nonsymbolic), we used leave-one-out cross-validation and normalized all firing rates by z-scoring (mean and standard deviation obtained from training data only) within each cross-validation repetition. For each classifier (n = 32), accuracy was assessed by counting the instances that a certain activity pattern was labeled correctly. To evaluate whether accuracy differed significantly from chance level (20% for five classes) when trained and tested at the same time points, we repeated the analysis with randomly shuffled trial labels (n_{perm} = 1000) and applied a cluster permutation test (p_{clus} = 0.01, p_{rank} = 1%; see *Sliding-Window 2-Factor ANOVA*). Finally, a multi-class SVM (with the same settings as above) was trained and tested on the firing rates obtained by averaging across the time window that was significant in the cross-training classification, i.e., window 780–1800 ms for the nonsymbolic number-units and 810–1370 ms for the symbolic number-cells (in cases where we obtained multiple significant windows, we used the onset of the first cluster and the offset of the last cluster as window boundaries). In addition to the overall accuracy, we assembled a confusion matrix which counted the frequency at which a trial of a certain stimulus class was assigned different labels by the classifier (main diagonal indicating correct labeling), and calculated the classification probabilities per numerical distance by averaging over the main and minor diagonals of the confusion matrix for each classifier (n = 32). Differences between adjacent classification probabilities were evaluated using Wilcoxon signed-rank tests (n = 32).

Population State-Space Analysis

For each unit, spike trains were averaged across conditions, normalized by z-scoring and smoothed (Gaussian kernel, σ = 50 ms, window size 300 ms). The temporal evolution of the neural activity of a population of *n* neurons can be represented as a trajectory in an *n*-dimensional space where each axis represents the instantaneous firing rate of one neuron. In our case, we analyzed the trajectories of the five different number conditions in a 92-dimensional space for the sub-population of nonsymbolic number-units, and in a 16-dimensional space for the symbolic number-units, respectively. To evaluate population tuning in terms of numerical distances, we calculated the Euclidean distances between each pair of trajectories, and averaged across those with the same numerical distance. This analysis was repeated with shuffled trial labels (n_{perm} = 1000) to obtain intertrajectory distances that would be expected for random numerical tuning, and evaluated using a cluster permutation test (p_{clus} = 0.01, p_{rank} = 1%; see *Sliding-Window 2-Factor ANOVA*). Solely for visualization purposes, trajectories were reduced to the top 3 (in terms of covariance they explain) orthonormalized dimensions using a Gaussian-process factor analysis (Yu et al., 2009).

Other Task Phases

Number-selectivity to operand 2 was assessed by performing a sliding-window 5-factor ANOVA with the factors 'numerical value' of operand 1 (1–5), 'numerical value' of operand 2 (0–5), 'protocol' (standard/ control), 'mathematical rule' (addition/ subtraction) and 'rule cue' (word/ symbol) for the operand 2 phase (analysis window 3050–3650 ms), separately for each format. We used the same parameters and procedures as for the operand 1 phases (see *Sliding-Window 2-Factor ANOVA*). A unit was counted as exclusively number-selective during the operand 2 phase if a significant cluster was observed between 3100–3400 ms (operand 2 onset to 200 ms before operand 2 offset) for the factor 'numerical value' of operand 2 and there were no overlapping significant clusters for any other factor. For the population of nonsymbolic number-units responsive to both operand 1 and 2 (n = 22) we calculated the preferred number per operand during the respective significant NUM-interval and quantified the relationship by calculating Pearson's linear correlation coefficient (see Figure S6). In addition, the significance of the proportion of units preferring the same number (k = 9) was evaluated using a binomial test (p_{chance} = 0.2 for five numbers).

Analogously, number-selectivity to the calculation result was determined for the delay 2 phase (analysis window 3550–4450 ms; we excluded the actual response phase in order to avoid confounds with motor responses) using a 6-factor ANOVA with the same factors as above, plus 'numerical value' of calculation result (0–9). Again, we used the same parameters and procedures as for the operand 1 phases (see *Sliding-Window 2-Factor ANOVA*) and counted a unit as exclusively number-selective if a significant cluster was observed between 3600–4200 ms (delay 2 onset to 200 ms before delay 2 offset) for the factor 'numerical value' of calculation result and there were no overlapping significant clusters for any other factor.

Furthermore, we determined rule-selective units by calculating a sliding-window 4-factor ANOVA with the factors 'mathematical rule' (addition/ subtraction), 'rule cue' (word/ symbol), 'numerical value' of operand 1 (1–5) and 'format' (symbolic/ nonsymbolic), thereby pooling over the factor 'protocol' (given its irrelevance for the processing of the rule cues), for the calculation rule and rule delay phases (analysis window 1750–3150 ms). The same parameters and procedures as for the operand 1 phases (see *Sliding-Window 2-Factor ANOVA*) were used. A unit was counted as exclusively rule-selective if a significant cluster was observed for the factor 'mathematical rule' between 1800–2900 ms (calculation rule onset to 200 ms before rule delay offset) and there were no overlapping significant clusters for any other factor. Exclusive cue-selectivity was defined analogously.

DATA AND SOFTWARE AVAILABILITY

Data and analysis software for this paper are available from the lead contact upon reasonable request.